Journal of Cerebral Blood Flow and Metabolism
10:740–747 © 1990 Raven Press, Ltd., New York

Graphical Analysis of Reversible Radioligand Binding from Time–Activity Measurements Applied to [*N*-^{11}C-methyl]-(−)-Cocaine PET Studies in Human Subjects

Jean Logan, Joanna S. Fowler, Nora D. Volkow, Alfred P. Wolf, Stephen L. Dewey, David J. Schlyer, Robert R. MacGregor, *Robert Hitzemann, Bernard Bendriem, S. John Gatley, and David R. Christman

*Department of Chemistry, Brookhaven National Laboratory, Upton, and *State University of New York at Stony Brook, Stony Brook, and Psychiatry Service, Veterans Administration Medical Center, Northport, New York, U.S.A.*

Summary: A graphical method of analysis applicable to ligands that bind *reversibly* to receptors or enzymes requiring the simultaneous measurement of plasma and tissue radioactivities for multiple times after the injection of a radiolabeled tracer is presented. It is shown that there is a time $t^{\dagger}$ after which a plot of $\int_0^t \mathrm{ROI}(t')dt'/\mathrm{ROI}(t)$ versus $\int_0^t C_p(t')dt'/\mathrm{ROI}(t)$ (where ROI and C_p are functions of time describing the variation of tissue radioactivity and plasma radioactivity, respectively) is linear with a slope that corresponds to the steady-state space of the ligand plus the plasma volume, V_p. For a two-compartment model, the slope is given by $\lambda + V_p$, where λ is the partition coefficient and the intercept is $-1/[k_2(1 + V_p/\lambda)]$. For a three-compartment model, the slope is $\lambda(1 + B_{max}/K_d) + V_p$ and the intercept is $-\{(1 + B_{max}/K_d)/k_2 + [k_{off}(1 + K_d/B_{max})]^{-1}\}\,[1 + V_p/\lambda(1 + B_{max}/K_d)]^{-1}$ (where B_{max} represents the concentration of ligand binding sites and K_d the equilibrium dissociation constant of the ligand–binding site complex, k_{off} (k_4) the ligand–binding site dissociation constant, and k_2 is the transfer constant from tissue to plasma). This graphical method provides the ratio B_{max}/K_d from the slope for comparison with in vitro measures of the same parameter. It also provides an easy, rapid method for comparison of the reproducibility of repeated measures in a single subject, for longitudinal or drug intervention protocols, or for comparing experimental results between subjects. Although the linearity of this plot holds when ROI/C_p is constant, it can be shown that, for many systems, linearity is effectively reached some time before this. This analysis has been applied to data from [*N-methyl*-^{11}C]-(−)-cocaine ([^{11}C]cocaine) studies in normal human volunteers and the results are compared to the standard nonlinear least-squares analysis. The calculated value of B_{max}/K_d for the high-affinity binding site for cocaine is 0.62 ± 0.20, in agreement with literature values. **Key Words:** Cocaine—PET—Graphical analysis—Transfer constants—Compartmental modeling—Receptors.

Positron emission tomography (PET) is an imaging method that allows sequential measurements of radioactivity in a region of interest (ROI) in vivo after an intravenous injection of a radiolabeled ligand. Several methods of analyzing PET data have been developed allowing comparisons to be made among experiments. One method is to assume a particular model in which a measured plasma input function governs the uptake of the labeled ligand. Model parameters can then be determined by a nonlinear least-squares (NLSQ) fit to the experimental data (see, for example, Carson, 1986). Graphical methods of analysis applicable to ligands that are trapped in tissue for the duration of the experiment have been developed and applied by several investigators (Gjedde, 1981; Patlak et al., 1983; Wong et al., 1984; Patlak and Blasberg, 1985; Gjedde et al., 1986). These methods are model independent and because of the simplicity of the calculation greatly facilitate the intercomparison of experimental data. Gjedde (1981) used a plot of $\mathrm{ROI}(t)/C_p(t)$ versus

Received October 6, 1989; revised February 14, 1990; accepted February 16, 1990.

Address correspondence and reprint requests to Dr. J. Logan at Chemistry Department, Brookhaven National Laboratory, Upton, NY 11973, U.S.A.

Abbreviations used: NLSQ, nonlinear least squares; PET, positron emission tomography; ROI, region of interest.

$\int_0^t C_p(t')\,dt'/C_p(t)$, which becomes linear for times in which the transport of radiotracer from plasma to tissue is unidirectional. This method was developed more formally by Patlak et al. (1983), who showed that when the reversible part of a system that contains at least one trapping mechanism approaches a steady state (at time $t\dagger$), such a plot becomes linear for times $t > t\dagger$. The slope and intercept can be related to the transport and binding constants of the ligand if a particular model is assumed. A variation of this presented by Patlak and Blasberg (1985) is a plot of $\mathrm{ROI}(t)/\mathrm{ROI}_{rv}(t)$ versus $\int_0^t \mathrm{ROI}_{rv}(t')\,dt'/\mathrm{ROI}_{rv}(t)$, where ROI_{rv} is the radioactivity from an ROI that does not contain the receptor or enzyme responsible for the irreversible trapping of the molecule. Wong (1984) introduced the plot of $\mathrm{ROI}(t)/\mathrm{ROI}_{rv}(t)$ versus time, which can also be shown to be linear in pertinent systems.

Many new radiotracers currently being introduced into PET are not trapped but have rapid dissociation constants and a rapid efflux from tissue. A graphical method of analysis applicable to such systems is presented here. This represents an extension to receptor systems of the linear analysis applied by Gjedde (1982) to a two-compartment system. As with the methods for irreversible trapping, no particular model structure is assumed. The method has been found to apply to PET data from [^{11}C]cocaine studies in humans in which the maximum radioactivity is achieved 5 to 10 min after injection with subsequent rapid washout.

THEORY AND METHODS

The kinetics of tracer amounts of labeled compounds in physiological systems can be described in terms of first-order, constant-coefficient, linear differential equations. The input function is generally a bolus injection of the labeled compound. The arterial plasma radioactivity can be described as the driving function of the differential equations that govern the uptake and loss of the tracer. The distribution of the tracer in tissue is described in terms of compartments that can be either a physical volume or a chemical volume (i.e., tracer bound to a receptor or enzyme). The time variation of the activity in multicompartment systems driven by an input function $C_p(t)$ can be described by (Patlak and Blasberg, 1985) (definitions of terms can be found in Appendix A)

$$d\mathbf{A}/dt = \mathbf{K}\mathbf{A} + \mathbf{Q}C_p(t) \tag{1}$$

where $\mathbf{A}$ is the column vector of concentrations (radioactivities) for each compartment at time t, $\mathbf{K}$ is the matrix of transfer constants, and $\mathbf{Q}$ is the vector describing transfer of activity from plasma to tissue (for the models considered here, the only nonzero element of $\mathbf{Q}$ is k_1). Patlak and Blasberg (1985) showed that Eq. (1) can be written as

$$\int_0^t A(t')\,dt' = -\mathbf{U}\mathbf{n}^T\mathbf{K}^{-1}\mathbf{Q}\int_0^t C_p(t')\,dt' + \mathbf{U}\mathbf{n}^T\mathbf{K}^{-1}\mathbf{A} \tag{2}$$

where $\mathbf{Un}^T$ is a row vector of 1s and $A(t) = \mathbf{U}\mathbf{n}^T\mathbf{A}$. Following Patlak, the total activity in the region of interest contains a contribution from the blood volume so that $\mathrm{ROI}(t) = A(t) + V_pC_p(t)$ (where V_p is the plasma volume within the ROI) and Eq. (2) becomes

$$\int_0^t \mathrm{ROI}(t')\,dt' = (-\mathbf{U}\mathbf{n}^T\mathbf{K}^{-1}\mathbf{Q} + V_p)\int_0^t C_p(t')\,dt' + \mathbf{U}\mathbf{n}^T\mathbf{K}^{-1}\mathbf{A} \tag{3}$$

Dividing Eq. (3) by $(\mathbf{U}\mathbf{n}^T\mathbf{A} + V_pC_p)$, we have a linear equation applicable to reversible systems when $\mathbf{U}\mathbf{n}^T\mathbf{K}^{-1}\mathbf{A}/[\mathbf{U}\mathbf{n}^T\mathbf{A} + V_pC_p(t)]$ becomes constant:

$$\frac{\int_0^t \mathrm{ROI}(t')\,dt'}{\mathrm{ROI}(t)} = (-\mathbf{U}\mathbf{n}^T\mathbf{K}^{-1}\mathbf{Q} + V_p)\frac{\int_0^t C_p(t')\,dt'}{\mathrm{ROI}(t)} + \frac{\mathbf{U}\mathbf{n}^T\mathbf{K}^{-1}\mathbf{A}}{\mathbf{U}\mathbf{n}^T\mathbf{A} + V_pC_p)} \tag{4}$$

Patlak et al. (1983) has shown that for $t > t\dagger$, $\mathbf{A} = -\mathbf{K}^{-1}\mathbf{Q}\,C_p(t)$ (the steady-state condition). When this is valid, the last term in Eq. (4) has reached its constant value so that after some time a plot of $\int_0^t \mathrm{ROI}(t')dt'/\mathrm{ROI}(t)$ versus $\int_0^t C_p(t')dt'/\mathrm{ROI}(t)$ is linear with slope $(-\mathbf{U}\mathbf{n}^T\mathbf{K}^{-1}\mathbf{Q} + V_p)$ and intercept $-\mathbf{U}\mathbf{n}^T\mathbf{K}^{-2}\mathbf{Q}/(-\mathbf{U}\mathbf{n}^T\mathbf{K}^{-1}\mathbf{Q} + V_p)$. Because the PET method measures the total radioactivity within an ROI, only a limited number of parameters can be uniquely determined from any given study. As a consequence of this, the models most frequently applied are the two- and three-compartment models shown below with transfer constants k_1, k_2, k_3, and k_4. When the three-compartment model refers to an enzyme or receptor system, the transfer constants can be related to the receptor (enzyme) parameters B_{max} (the concentration of radiotracer binding sites), K_d (the equilibrium dissociation constant for the radiotracer–binding site complex), k_{off} (the ligand–binding site dissociation constant), and k_{on} (the ligand–binding site association constant). In this case, $k_3 = B_{max}\,k_{on}$, $k_4 = k_{off}$, $k_3/k_4 = B_{max}/K_d$, and $K_d = k_{off}/k_{on}$. In terms of the two-compartment model (one tissue compartment with ligand concentration C_1 plus the input function C_p), the slope of Eq. (4) becomes $\lambda + V_p$, where λ is the partition coefficient (k_1/k_2) and the intercept is $-1/[k_2(1 + V_p/\lambda)]$. For the three-compartment model (two tissue compartments, where C_2 corresponds to a ligand bound to a receptor or enzyme), the slope is $[\lambda(1 + B_{max}/K_d) + V_p]$, which can also be expressed in terms of transfer constants as $[k_1/k_2(1 + k_3/k_4 + V_p)]$ (It is assumed that the specific activity is sufficiently high so that the number of free binding sites is approximately equal to B_{max}):

two-compartment model

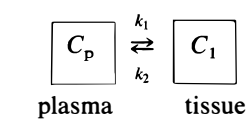

plasma tissue

three-compartment model

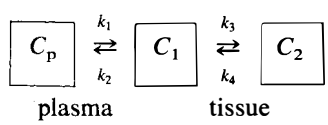

plasma tissue

For comparison to the graphical method presented here, the model constants were also determined using a nonlinear fitting technique. The model equations were solved numerically using a modified divided difference form of the Adams–Pece formula (Shampine and Gordon, 1975). Optimum values of the model parameters were found by a simplex search method (Press et al., 1986) minimizing the sum of the squared differences between the measured PET value and the model prediction using a correction for the contribution of the blood volume to the total activity. The input function (plasma activity) was corrected for the presence of the metabolites of cocaine (Fowler et al., 1989). The sensitivity matrix was computed and standard errors of the model parameters were estimated from the diagonal elements of the covariance matrix (Carson, 1986). In all cases, the ratio k_1/k_2 was fixed at the value found for the cerebellum.

Both the graphical and nonlinear least squares (NLSQ) analyses were applied to data from PET studies on four normal male volunteers (age range of 26–46 years) receiving tracer doses of ^{11}C-labeled cocaine ([*N*-^{11}C]-(−)-cocaine) (6.5–10 mCi, 9–13 μg per injection). A second study on each individual was repeated at 2–3 h intervals after the first injection to test reproducibility and to set the stage for drug intervention studies. Arterial plasma samples were taken throughout the experiment for both studies and selected samples were analyzed for unchanged [^{11}C]cocaine (for experimental details, see Fowler et al., 1989).

RESULTS AND DISCUSSION

Table 1 contains the results for the graphical analysis technique. Figure 1A illustrates the model fit to time activity data for ROIs from striatum and cerebellum. Figure 1B is a typical example illustrating the graphical analysis applied to ROIs from the cerebellum and the striatum (subject D1). The linear region begins at about 8 min after injection. The slope is greatest for the ROI from the striatum. Cocaine binds principally to the dopamine transporter complex, which is present on the presynaptic dopaminergic neuron in the striatum (Kennedy and Hanbauer, 1983). Assuming that the cerebellum corresponds to the two-compartment model shown above and the striatum to the three-compartment model in which C_2 represents the receptor–ligand complex, the receptor parameter B_{max}/K_d (k_3/k_4) can be determined from this analysis (see Table 2). Neglecting V_p (plasma volume), which is on the order of 3–4% of brain tissue (Phelps et al., 1979), and therefore represents a small contribution to the values given in Table 1, B_{max}/K_d can be determined from the ratio of slopes for the two ROIs (assuming λ is the same for both regions). These results are reported in Table 3. The variation in the slopes reported in Table 1 between studies 1 and 2 was remarkedly small, the largest being 11%. A greater variability in B_{max}/K_d was observed (Table 2). This is not unexpected since B_{max}/K_d is obtained from the ratio of two values, each of which contains errors and suggests that a better comparison might be the slope itself as long as the transport parameters k_1 and k_2 have not been altered.

A comparison of the transport constants k_1 and k_2 and their ratio λ obtained from a nonlinear least-squares fit using the two-compartment model for the cerebellum with results from the graphical analysis are presented in Table 3. The results are in agreement, indicating that the graphical method

TABLE 1. *Slopes and intercepts from the graphical analysis of data from repeated PET studies with [^{11}C]cocaine in human subjects*

Subject	Study	ROI	Slope	% Change	Intercept
A	1	Striatum	3.49		−7.97
A	2	Striatum	3.14	11.1	−5.9
A	1	Cerebellum	2.01		−3.3
A	2	Cerebellum	2.04	−1.5	−3.6
B	1	Striatum	5.64		−11.0
B	2	Striatum	5.38	4.6	−10.0
B	1	Cerebellum	3.54		−6.5
B	2	Cerebellum	3.72	−5.1	−7.4
C	1	Striatum	6.62		−10.6
C	2	Striatum	6.12	7.6	−10.7
C	1	Cerebellum	3.45		−6.6
C	2	Cerebellum	3.25	5.8	−6.1
D	1	Striatum	4.60		−7.7
D	2	Striatum	4.40	4.3	−7.8
D	1	Cerebellum	3.30		−5.4
D	2	Cerebellum	3.09	6.3	−5.5

For each subject, there was a 2–3 h interval between study 1 and study 2. The % variation in the slope between studies is reported as (study 1 − study 2)/study 1.

The equation of analysis is $\int_0^t \mathrm{ROI}(t')dt'/\mathrm{ROI}(t)$ = slope $\int_0^t C_p(t')dt'/\mathrm{ROI}(t)$ + intercept for experimental scan times t such that $t > t^*$. For a two-compartment model, the slope is $\lambda + V_p$ and the intercept is $-1/[k_2(1 + \lambda V_p)]$ ($\lambda = k_1/k_2$). For a three-compartment model, the slope becomes $[\lambda(1 + B_{max}/K_d) + V_p]$, where $B_{max}/K_d = k_3/k_4$.

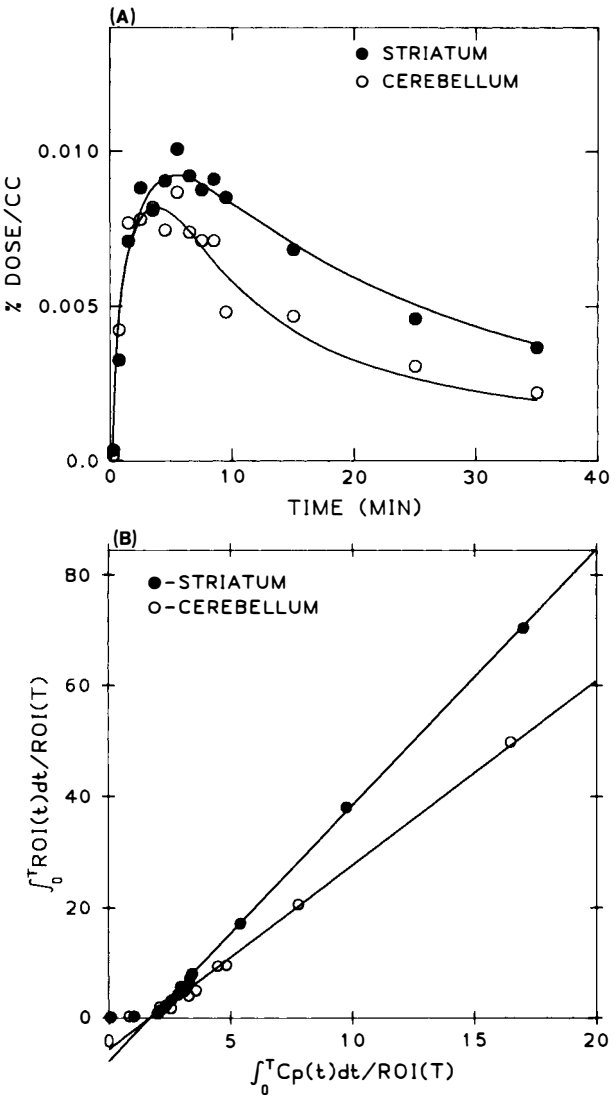

FIG. 1. (A) Time—activity data from striatum and cerebellum ROIs from a PET study with[^{11}C]cocaine in a human volunteer. The solid lines are the two- and three-compartment model fits for the cerebellum and striatum using the arterial plasma activity (corrected for the presence of labeled cocaine metabolites) as the input function. The points on the graph are calculated for the midpoint of the scan times represented by *T*. ROI refers to radioactivity in the regions of interest. **(B)** Graphical analysis of the time activity data from striatum and cerebellum ROIs. ROI(*T*) refers to radioactivity in the region of interest at time *T*. $C_p(t)$ is the plasma radioactivity corrected for metabolites. Data are from subject D1.

provides essentially the same information as the model fit. The ratios k_3/k_4 (B_{max}/K_d) are also compared for the two methods. The model parameters k_3 and k_4 were determined individually using the NLSQ method; however, the standard errors were very large even though the ratios k_3/k_4 were found to be stable. This dependence upon the ratio but not the individual values of the binding parameters is illustrated in Fig. 2. The ratio was fixed at 0.77 while the value of k_4 was varied from 0.4 (lower curve) to 1.6 min^{-1} (upper curve), with little change in the resulting curves. This insensitivity to changes in k_4 can occur when k_4 is much greater than k_2. The total tissue activity can be written in terms of the eigenvalues ($\alpha_\pm$) and the coefficients ($\gamma_{1,2}$) (see Table 4 and the appendices) as $k_1(\gamma_1 e^{\alpha_+ t} + \gamma_2 e^{\alpha_- t}) \otimes C_p(t)$, where $\otimes$ denotes convolution. When $k_4 \gg k_2$,

$$\alpha_+ \rightarrow -\frac{k_2}{2}\left(1 - \frac{k_3/k_4 - 1}{k_3/k_4 + 1}\right)$$

and

$$\alpha_- \rightarrow -(k_3 + k_4) - \frac{k_2}{2}\left(1 + \frac{k_3/k_4 - 1}{k_3/k_4 + 1}\right)$$

In this case, α_+ depends only on k_2 and the ratio k_3/k_4. Table 4 gives the variation in the eigenvalues and the coefficients for a range of values of k_4 with $k_3/k_4 = 0.77$ using fixed values of k_1 and k_2. When $k_4 = 0.8$ with $k_2 = 0.23$, there is little further change in α_+ or γ_1. The γ_2 term makes a much smaller contribution to the total radioactivity. (Note that without prior knowledge of k_1 and k_2 or their ratio from the cerebellum, the activity in the striatum would appear to be a two-compartment model. The ratio k_3/k_4 can only be determined if k_1/k_2 is known.)

In theory, k_4 (k_{off}) can also be determined from the intercept of the graphical method given by

$$-\left(\frac{1 + B_{max}/K_d}{k_2} + \frac{1}{k_{off}(1 + K_d/B_{max})}\right)$$

neglecting the correction for V_p. However, for the

TABLE 2. *Receptor parameters determined from the ratio of striatum slope to cerebellum slope.*

Subject	Study	Ratio of slopes	B_{max}/K_d[a]
A	1	1.74	0.74
A	2	1.54	0.54
B	1	1.59	0.59
B	2	1.45	0.45
C	1	1.92	0.92
C	2	1.88	0.88
D	1	1.39	0.39
D	2	1.42	0.42
Mean		1.62 ± 0.21	0.62 ± 0.21

It is assumed that the cerebellum corresponds to a two-compartment model and the striatum corresponds to a three-compartment model so that ratio of slopes is $(1 + B_{max}/K_d)$ or $(1 + k_3/k_4)$, neglecting V_p, which is generally on the order of 0.04 and therefore small compared to the slopes reported here.

Assuming a 4% blood volume in both cerebellum and striatum, the average value of B_{max}/K_d was calculated to be 0.624.

[a] Neglecting V_p; $B_{max}/K_d = k_3/k_4$.

TABLE 3. *Comparison of parameters determined by graphical analysis with those determined from a nonlinear least-squares model fit*

Subject	Study	λ^a	λ^b	$k_1{}^a$	$k_2{}^a$	$k_1{}^b$	$k_2{}^b$	$B_{max}/K_d{}^a$	$B_{max}/K_d{}^b$
A	1	2.01	2.02	0.61	0.30	0.46	0.23	0.74	0.78
A	2	2.04	1.97	0.57	0.28	0.47	0.24	0.54	0.52
B	1	3.54	3.18	0.54	0.15	0.52	0.16	0.59	0.75[c]
B	2	3.70	3.37	0.50	0.14	0.56	0.17	0.45	0.60[c]
C	1	3.45	3.42	0.52	0.15	0.49	0.14	0.92	0.93
C	2	3.25	3.10	0.53	0.16	0.52	0.17	0.88	0.95
D	1	3.30	3.44	0.61	0.19	0.51	0.15	0.39	0.43
D	2	3.09	3.0	0.56	0.18	0.54	0.18	0.42	0.40
Mean								0.62 ± 0.21	0.66 ± 0.21

The kinetic constants k_1 and k_2 are in units of min^{-1} and $\lambda = k_1/k_2$, $B_{max}/K_d = k_3/k_4$.
[a] Determined with the graphical method from the cerebellum.
[b] Determined using a nonlinear least-squares fit to the cerebellum.
[c] The large difference in B_{max}/K_d is due to the difference in λ.

reasons discussed above, k_4 could not be accurately determined for cocaine.

Schoemaker et al. (1985) determined a high-affinity component to cocaine binding in postmortem human putamen with K_d of 0.21 μmol/L and a B_{max} of 1.47 pmol/mg of protein. Assuming 10% protein per cc of tissue, this translates into ≈0.7 for B_{max}/K_d, which is in agreement with the values reported here (0.62 ± 0.20). Shoemaker et al. (1985) also report a low-affinity component to the binding. However, it was not possible to separate another binding component from the PET data using the nonlinear least-squares method or the graphical method.

Frost et al. (1989) report a multicompartment analysis of [^{11}C]carfentanil binding in PET studies of human subjects. Carfentanil is a reversible ligand that binds to μ opiate receptors. They were able to determine individual values for the receptor constants k_3 and k_4 but the values found for k_4 were not significantly different from the values for k_2 as opposed to $k_4 \gg k_2$ as seems to be the case for cocaine. They also found that a three-compartment model was required to describe binding in the occipital cortex, which has a negligible concentration of opiate receptors. They suggest that the third compartment represents nonspecific binding that does not rapidly equilibrate with the free ligand, as is the usual assumption (Mintun et al., 1984; Logan et al., 1987). The cocaine data reported here for humans did not require the extra compartment for nonreceptor regions although the cocaine data from studies in baboons did require such a model (Logan et al., 1989). One major difference between the baboon and human data is that the disappearance of labeled cocaine from baboon plasma was significantly faster than from human plasma and baboon plasma contained significant amounts of labeled carbon dioxide whereas human plasma did not. A

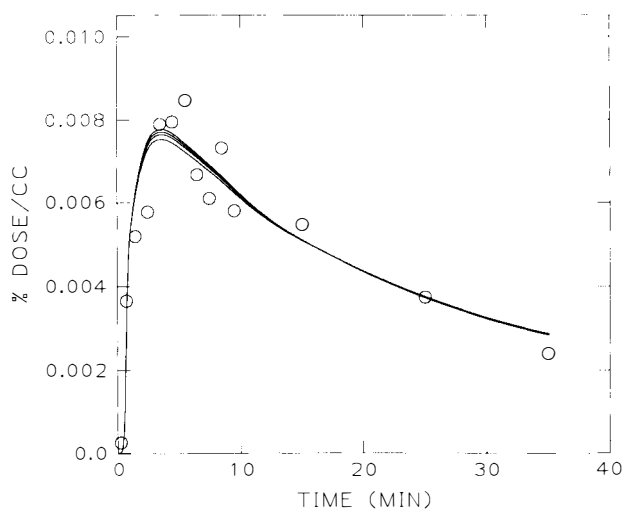

FIG. 2. Variation in the three-compartment model fit to tissue activity using a fixed value of k_3/k_4 while varying k_4 from 0.399 min^{-1} (lower curve) to 1.60 min^{-1} (upper curve). The ratio was fixed at 0.77. The parameter values are given in Table 4. Data are from subject A1.

TABLE 4. *Variation in the eigenvalues and coefficients of the analytical solution for the three-compartment model for a fixed ratio of k_3/k_4 with increasing values of k_4 (λ = 2.0, k_2 = 0.23).*

k_3	k_4	α_+	α_-	γ_1	γ_2
0.307	0.399	−0.111	−0.825	0.425	0.119
0.614	0.797	−0.121	−1.520	0.922	0.078
0.921	1.196	−0.124	−2.223	0.949	0.051
1.228	1.595	−0.125	−2.928	0.963	0.037

The solution for the tissue activity of the three-compartment model considered is $C_1 + C_2 = k_1(\gamma_1 e^{\alpha_+ t} + \gamma_2 e^{\alpha_- t}) \otimes C_p(t)$, where $\gamma_1 = (k_3 + k_4 + \alpha_+)/(\alpha_+ - \alpha_-)$ and $\gamma_2 = -(k_3 + k_4 + \alpha_-)/(\alpha_+ - \alpha_-)$. Since k_4 becomes much greater than k_2, there is little variation in either γ_1 or α_+ while the contribution from the γ_2 term becomes increasingly small. For this reason, the curves in Fig. 2 (data are from subject A1) do not change very much since k_4 is increased by a factor of 4. The ratio of k_3/k_4 was fixed at 0.77.

second difference is that the baboon studies were done with anesthetic (Fowler et al., 1989).

The graphical technique presented here depends upon the constancy of the last term of Eq. (4), i.e., the intercept. The expression for the intercept when it has reached its constant (steady-state) value is $-\mathbf{U}\mathbf{n}^T\mathbf{K}^{-2}\mathbf{Q}/(-\mathbf{U}\mathbf{n}^T\mathbf{K}^{-1}\mathbf{Q} + V_p)$, which is obtained by substituting for $\mathbf{A}$ its steady-state value, $\mathbf{A} = -\mathbf{K}^{-1}\mathbf{Q}\,C_p(t)$ [$A(t)/C_p$ = constant]. Surprisingly, in this case, the slope shows little variation even when very early times are included in the calculation, while the variation in $A(t)/C_p$ (see Table 5) is much greater. This suggests that under certain conditions, the ratio of terms in the intercept effectively reaches the steady-state value before $A(t)/C_p$. We have investigated the variation of the intercept as the system approaches the steady state using the specific example of the three-compartment model. In general, the condition for which $\mathbf{A} = -\mathbf{K}^{-1}\mathbf{Q}\,C_p(t)$ depends upon the eigenvalues of the system such that $e^{\alpha_\pm t} \to 0$ and $|\alpha_\pm| \gg$ the smallest exponent, β_q describing plasma activity. It is assumed that C_p can be represented as a sum of exponentials $C_p = \Sigma_k B_k e^{-\beta_k t}$. Immediately following a bolus injection, plasma levels decline rapidly, characterized by large values for the exponent β_k. However, after 2 to 3 min, the plasma levels decline much more slowly and can be represented by a small exponent, $C_p \to B_q\, e^{-\beta_q t}$. (See Patlak et al., 1983, p. 4 for a discussion concerning steady-state conditions.) We will consider here the situation some time before the steady-state limit is reached. The exact expression for the intercept of the three-compartment model is given by

$$\frac{\mathbf{U}\mathbf{n}^T\mathbf{K}^{-1}\mathbf{A}}{C_1 + C_2 + V_pC_p} = -\left[\frac{1}{k_2}\left(1 + \frac{B_{max}}{K_d}\right) + \frac{C_2}{k_4(C_1 + C_2)}\right]\left[\frac{1}{1 + V_pC_p/(C_1 + C_2)}\right] \quad (5)$$

Neglecting $V_pC_p/(C_1 + C_2)$ since it is much less than 1 (the plasma volume could also be approximated from literature values so that the plasma contribution to the total activity can be subtracted from the data prior to analysis), the only time variation appears in $C_2/(C_1 + C_2)$, which goes to $1/(1 + K_d/B_{max})$ in the steady state. From simulation studies presented in Table 5, the theoretical value of $C_2/(C_1 + C_2)$ calculated from model parameters is within 2% of its steady-state value at 7 min after injection, while the value calculated for $(C_1 + C_2)/C_p$ at 8 min postinjection differs significantly from its steady-state value (see Table 5). A comparison of the analytical expressions for $C_2/(C_1 + C_2)$ and $(C_1 + C_2)/C_p$ provides some insight into why the former appears to reach its steady-state value before the latter. Equations (B3), (B4), and (B6) derived in Appendix B indicate how these terms approach their steady-state value. (See Appendix A for definitions of $\alpha_\pm$.) Neglecting β_q in Eq. (B3) since $\beta_q \ll 1$, the correction terms in Eqs. (B3), (B4), and (B6) contain the parameter ω [defined in Eq. (B5)], which determines how fast these terms reach their steady-state value. Since $\alpha_+ < 0$, $\omega \to 0$ for t sufficiently large, the limiting value for $(C_1 + C_2)/C_p$ from Eq. (B3) is $k_1k_4(1 + B_{max}/K_d)/(\alpha_+ + \beta_q)(\alpha_- + \beta_q)$. This goes to the true steady state limit $\lambda(1 + B_{max}/K_d)$ only when $\alpha_+ + \beta_q \approx \alpha_+$ and $\alpha_- + \beta_q \approx \alpha_-$, i.e., when plasma activity is constant or the exponent describing the plasma activity is small compared to the eigenvalues of the system. However, for $C_2/(C_1 + C_2)$ since there are no terms involving $(\alpha_\pm + \beta_q)$, the limiting value is $1/(1 + K_d/B_{max})$. Furthermore from the form of the correction terms, the terms containing ω in Eqs. (B3), (B4), and (B6), $C_2/(C_1 + C_2)$ will be closer to its steady-state value than will $(C_1 + C_2)/C_p$ when $|\alpha_+/(k_3 + k_4)|$ is small ($\approx$0.25 or less) even though ω differs significantly from 0. The model parameters found for cocaine predict that the absolute value of $|\alpha_+/(k_3 + k_4)|$ is less than 0.1. Consider for example that it has the value -0.1 with $\omega = 2$. The correction terms for Eqs. (B3) and (B6) are 1.8 and 0.07, respectively, so that $C_2/(C_1 + C_2)$ differs from its steady-state value by 7% while $(C_1 + C_2)/C_p$ is 2.8 times greater than its steady-state value. For such systems, one expects that this

TABLE 5. *Graphical method of Eq. (4) applied to simulation data generated from a three-compartment model using an experimental input function (subject A2) with 4% blood volume*

T_i[a] (min)	T_f[a] (min)	Slope	T[b] (min)	ROI/C_p
4	35	3.51	4	4.63
6	35	3.51	6	5.18
8	35	3.51	8	5.61
10	35	3.51	10	5.79
15	35	3.51	15	4.83
			35	4.33
			55	4.05

The kinetic constants used in the simulation were similar to those found for the striatal ROI in the [^{11}C]cocaine studies (k_1 = 0.48, k_2 = 0.24, k_3 = 0.5, k_4 = 0.67 in units of min^{-1}) and predict a slope of 3.51. Including very early times in the calculation of the slope does not affect the outcome even though the variation in ROI/C_p is substantial over these times. ROI/C_p approaches the same value as the slope when C_p is constant. When C_p is not constant, ROI/$C_p \to k_1(k_3 + k_4)/[(\alpha_+ + \beta_q)(\alpha_- + \beta_q)]$, which is larger than the slope. The contribution from the term $V_pC_p/(C_1 + C_2)$ varied from 0.01 to 0.03 and therefore should have no noticeable effect on the results.

[a] Data points falling between the initial time T_i and the final time T_f were used in computing the slope.

[b] Times for which ROI/C_p were computed.

method will yield reasonably accurate results even before $A(t)/C_p$ has reached its steady-state value.

CONCLUSIONS

We have presented a technique for the analysis of time–activity data from PET studies with ligands characterized by rapid transport and dissociation constants so that their uptake and loss by tissue is clearly observable during the course of the experiment. We have compared results from this technique with model parameter estimates based on a NLSQ method for the analysis of [^{11}C]cocaine PET studies in human subjects. Results from both methods were in agreement and the values obtained for B_{max}/K_d are consistent with in vitro work. It was not possible to determine separately the receptor parameters (k_3 and k_4) but this is most likely due to the fact that $k_4 \gg k_2$. The graphical technique is easier to apply than the standard nonlinear least-squares method of fitting an explicit model to experimental data particularly when unique values cannot be determined for the model parameters with an NLSQ method and is valid when $\mathbf{U}\mathbf{n}^T\mathbf{K}^{-1}\mathbf{A}/[\mathbf{U}\mathbf{n}^T\mathbf{A} + V_pC_p(t)]$ becomes constant [certainly true when $A(t)/C_p$ is constant but depending on the kinetic parameters of the system may be true well before that time]. Whether this method can be applied is best determined by plotting $\int_0^t \mathrm{ROI}(t')dt'/\mathrm{ROI}(t)$ versus $\int_0^t C_p(t')dt'/\mathrm{ROI}(t)$ and observing whether or not the plot is linear after some time. For the two-compartment model it will be linear at all times. The slope corresponds to the plasma volume plus the steady-state space of the ligand, which for a two-compartment model is given by $\lambda + V_p$ and for a three-compartment model is $[\lambda(1 + B_{max}/K_d) + V_p]$. This is also given by the true steady-state limit of ROI/C_p that is attained when the smallest exponent describing the plasma levels is much less than the eigenvalues of the system and also corresponds to the intercept of the traditional Patlak plot, which has a 0 slope for reversible ligands and an intercept equal to ROI/C_p. The intercepts from the graphical method described here are $-1/[k_2(1 + V_p/\lambda)]$ for the two-compartment model and

$$-\left(\frac{1 + B_{max}/K_d}{k_2} + \frac{1}{k_{off}(1 + K_d/B_{max})}\right)\frac{1}{1 + V_p/\lambda(1 + B_{max}/K_d)}$$

for the three-compartment model. This technique provides a more reliable measure of the steady-state space and also allows two measurements, the slope and the intercept, so that in theory model parameters can be explicitly determined although it may be necessary to correct for the plasma volume. The presence of a tissue component with a long half-life will result in an increasing slope so that this method is not valid. The presence of such a component can be determined from the traditional Patlak plot.

Acknowledgments: This work was carried out at Brookhaven National Laboratory under contract DE-AC02-76CH00016 with the U.S. Department of Energy and supported by its Office of Health and Environmental Research. We also acknowledge partial support from the National Institutes of Health (Grant NS-15638). We are grateful to the National Institute on Drug Abuse for samples of norcocaine and (−)-cocaine. We are particularly grateful to P. King, K. Karlstrom, E. Jellett, and C. Shea for their assistance in radiotracer preparation and analysis, to R. Moadel for PET operations, and to N. Netusil and T. Johnson for patient preparation and supervision. We also thank D. Warner, C. Barrett, and R. Carciello for cyclotron operations.

APPENDIX A: DEFINITIONS

$\mathbf{A}$	Vector of activities for a compartmental model
$A(t)$	Sum of activities
$\mathbf{K}$	Matrix of transfer constants for a compartmental model for the three compartment model, $\mathbf{K} = \begin{pmatrix} -(k_2 + k_3) & k_4 \\ k_3 & -k_4 \end{pmatrix}$
$\mathbf{Q}$	Vector of constants describing transport from plasma to tissue
ROI	Total activity in a region of interest including plasma activity
V_p	Plasma volume in 1 cc of tissue
C_p	Activity in plasma due to unchanged drug
k_1	Transfer constant from plasma to tissue (min^{-1})
k_2	Transfer constant from tissue to plasma (min^{-1})
k_3	$k_{on}B_{max}$
k_4	Dissociation constant for ligand–binding site complex = k_{off}
B_{max}	Receptor (binding site) concentration
k_{on}	Bimolecular association constant for radiotracer and binding site, in units of cc/pmol · min^{-1}
k_{off}	Dissociation constant for ligand–binding site complex (min^{-1}) = k_4
K_d	Equilibrium dissociation constant for ligand-binding-site complex (k_{off}/k_{on})
B_{max}/K_d	$= k_3/k_4 = k_{on}B_{max}/k_{off}$
C_1	Tissue activity in the two- or three-compartment model that is not bound to receptor or enzyme
C_2	Tissue activity in the three-compartment model that is associated with receptor or enzyme
λ	Partition coefficient for the ligand k_1/k_2
$\alpha_\pm$	Eigenvalues for the three-compartment model: $\frac{1}{2}[-K \pm (K^2 - 4k_2k_4)^{1/2}]$, $K = k_2 + k_3 + k_4$

γ_1 $(k_3 + k_4 + \alpha_+)/(\alpha_+ - \alpha_-)$
γ_2 $-(k_3 + k_4 + \alpha_-)/(\alpha_+ - \alpha_-)$

APPENDIX B

The solution to Eq. (1) for the three-compartment model is

$$C_1 + C_2 = k_1(\gamma_1 e^{\alpha_+ t} + \gamma_2 e^{\alpha_- t}) \otimes C_p(t) \quad \text{(B1)}$$

where ($\alpha_\pm$) are the eigenvalues of the system (see Appendix A for definitions of $\alpha_\pm$ and $\gamma_{1,2}$) and $\otimes$ denotes convolution. As the steady state is approached, plasma levels from the bolus injection approach a slow monoexponential decline, i.e.,

$$C_p = \sum_k B_k e^{-\beta_k t} \rightarrow B_q e^{-\beta_q t}$$

where β_q is the smallest exponent (and therefore the most important one at later times). The B_k and β_k are constants. (In the true steady-state limit, $e^{\alpha_\pm t} \rightarrow 0$ and $\alpha_\pm \gg \beta_q$ so that $\mathbf{A} = -\mathbf{K}^{-1}\mathbf{Q}\,C_p$.) Also, as the steady state is approached, terms involving $e^{\alpha_- t} \rightarrow 0$ faster than terms containing $e^{\alpha_+ t}$ since $|\alpha_-| > |\alpha_+|$. Under these conditions, the most important terms remaining after the convolutions in Eq. (B1) are

$$e^{\alpha_+ t} \otimes C_p(t) \rightarrow e^{\alpha_+ t}\rho_+ - \frac{C_p}{\alpha_+ + \beta_q} \quad \text{(B2)}$$

$$e^{\alpha_- t} \otimes C_p(t) \rightarrow -\frac{C_p}{\alpha_- + \beta_q}$$

This leads to

$$\frac{(C_1 + C_2)}{C_p} = \frac{k_1 k_4\left(1 + \frac{B_{max}}{K_d}\right)}{(\alpha_+ + \beta_q)(\alpha_- + \beta_q)}\left[1 + \omega\left(\frac{\alpha_+}{k_3 + k_4} + 1\right) - \frac{\beta_q}{k_3 + k_4}\right] \quad \text{(B3)}$$

$$\frac{C_2}{C_p} = \frac{k_1 k_3}{(\alpha_+ + \beta_q)(\alpha_- + \beta_q)}(1 + \omega) \quad \text{(B4)}$$

where

$$\omega = \frac{e^{\alpha_+ t}\rho_+}{C_p}\left(\frac{(\alpha_+ + \beta_q)(\alpha_- + \beta_q)}{a_+ - \alpha_-}\right) \quad \text{(B5)}$$

$$\rho_+ = \sum_k \frac{B_k}{\alpha_+ + \beta_k}$$

so that

$$\frac{C_2}{C_1 + C_2} \rightarrow \frac{1}{1 + K_d/B_{max}}\left(1 - \frac{\omega\alpha_+/(k_3 + k_4)}{1 + \omega[\alpha_+/(k_3 + k_4) + 1]}\right) \quad \text{(B6)}$$

The true steady-state limit (steady-state space) is

$$\frac{C_1 + C_2}{C_p} = \frac{k_1(k_3 + k_4)}{k_2 k_4} = \lambda\left(1 + \frac{B_{max}}{K_d}\right)$$

$$C_2/C_p = \frac{k_1 k_3}{k_2 k_4} = \lambda\frac{B_{max}}{K_d}$$

which is true when $\beta_q \ll \alpha_+, \alpha_-$.

REFERENCES

Carson RE (1986) Parameter estimation in positron emission tomography. In: *Positron Emission Tomography and Autoradiography: Principles and Applications for the Brain and Heart* (Phelps M, Mazziotta, Schelbert H, eds), New York, Raven Press, pp 347–390

Fowler J, Volkow ND, Wolf AP, Dewey SL, Schlyer DJ, MacGregor RR, Hitzemann R, Logan J, Bendriem B, Gatley J, Christman D (1989) Mapping cocaine binding sites in human and baboon brain *in vivo*. *Synapse* 4:371–377

Frost JJ, Douglas KH, Mayberg HS, Dannals RF, Links JM, Wilson AA, Ravert HT, Crozier WC, Wagner HN Jr (1989) Multicompartmental analysis of ^{11}C-carfentanil binding to opiate receptors in humans measured by positron emission tomography. *J Cereb Blood Flow Metab* 9:398–409

Gjedde A (1981) High- and low-affinity transport of D-glucose from blood to brain. *J Neurochem* 36:1463–1471

Gjedde A (1982) Calculation of cerebral glucose phosphorylation from the brain uptake of glucose analogs in vivo: a re-examination. *Brain Res* 4:237–274

Gjedde A, Wong DF, Wagner HN Jr (1986) Transient analysis of irreversible and reversible tracer binding in human brain *in vivo*. In: *PET and NMR: New Perspectives in Neuroimaging and in Clinical Neurochemistry* (Battistin L, ed), New York, Alan R. Liss, pp 223–235

Kennedy LT, Hanbauer I (1983) Sodium-sensitive cocaine binding to rat striatal membrane: possible relationship to dopamine uptake sites. *J Neurochem* 41:171–178

Logan J, Wolf AP, Shiue CY, Fowler JS (1987) Kinetic modeling of receptor–ligand binding applied to positron emission tomographic studies with neuroleptic tracers. *J Neurochem* 48:73–87

Logan J, Fowler JS, Dewey SL, Wolf AP, Volkow ND, Christman DR, MacGregor R, Schlyer DJ, Bendriem B (1989) Kinetic analysis of PET studies with ^{11}C-cocaine in the baboon brain. *J Nucl Med* 30:898

Mintun MA, Raichle ME, Kilbourn MR, Wooten GF, Welch MJ (1984) A quantitative model for the *in vivo* assessment of drug binding sites with positron emission tomography. *Ann Neurol* 15:217–227

Patlak CS, Blasberg RG, Fenstermacher JD (1983) Graphical evaluation of blood-to-brain transfer constants from multiple-time uptake data. *J Cereb Blood Flow Metab* 3:1–7

Patlak CS, Blasberg RG (1985) Graphical evaluation of blood-to-brain transfer constants from multiple-time uptake data. Generalizations. *J Cereb Blood Flow Metab* 5:584–590

Phelps ME, Huang SC, Hoffman EJ, Kuhl DE (1979) Validation of tomographic measurement of cerebral blood volume with ^{11}C labeled carboxyhemoglobin. *J Nucl Med* 20:328–334

Press WH, Flannery BP, Teukolsky SA, Vetterling WT (1986) *Numerical Recipes. The art of Scientific Computing*. Cambridge, Cambridge University Press

Schoemaker H, Pimoule C, Arbilla S, Scatton B, Javoy-Agid F, Langer SZ (1985) Sodium dependent [^{3}H]cocaine binding associated with dopamine uptake sites in the rat striatum and human putamen decrease after dopaminergic denervation and in Parkinsons disease. *Naunyn Schmiedebergs Arch Pharmacol* 329:227–235

Shampine LF, Gordon MK (1975) *Computer Solution of Ordinary Differential Equations: The Initial Value Problem*. San Francisco, W.H. Freeman, pp 289–293

Wong DF, Wagner HN Jr., Dannals RF, Links JM, Frost JJ, Ravert HT, Wilson AA, Rosenbaum AE, Gjedde A, Douglass KH, Petronis JD, Folstein JK, Toung JKT, Burns HD, Kuhar MJ (1984) Effects of age on dopamine and serotonin receptors measured by positron tomography in the living human brain. *Science* 226:1393–1396